

Effects of surface roughness and oscillatory flow on the dissolution of plaster forms: Evidence for nutrient mass transfer to coral reef communities

James L. Falter¹ and Marlin J. Atkinson

Hawaii Institute of Marine Biology, Kaneohe, Hawaii 96744

Carlos F. M. Coimbra

Department of Mechanical Engineering, University of Hawaii, Manoa, Hawaii 96822

Abstract

We dissolved plaster forms in seawater to examine the effects of surface roughness and flow conditions on mass-transfer rates. Plaster blocks with varying roughness were dissolved under both steady and oscillatory flows between 7 and 43 cm s⁻¹ yielding calcium mass-transfer coefficients (S_{Ca}) that varied from 0.5 to 3 m d⁻¹. S_{Ca} measured in a flume was 30–40% greater under oscillatory flow than under steady flow at flow speeds <10 cm s⁻¹; this difference decreased with increasing flow speed. Plaster blocks with added millimeter-, centimeter-, and decimeter-scale roughness were dissolved under oscillatory flows between 2 and 26 cm s⁻¹ on three different coral reef flats. Plaster dissolution rates in the field were linearly proportional to surface area regardless of the roughness scale. Variation in S_{Ca} across different reef environments was less affected by whether the flow was steady or oscillatory (a factor of 1.2–1.6) than it was by flow speed alone (a factor of 4.7).

Water motion is an important factor regulating the exchange of metabolites between reef communities and their surrounding environment. Rates of nutrient uptake (Atkinson and Bilger 1992; Thomas and Atkinson 1997), photosynthetic production (Dennison and Barnes 1988; Carpenter et al. 1991), and nitrogen fixation (Williams and Carpenter 1988; Carpenter et al. 1991) by coral and algae increase with greater water motion. This occurs as a result of changes in the rate at which dissolved compounds are physically transferred across concentration boundary layers adjacent to the surfaces of autotrophic organisms. Prior studies of metabolite mass transfer have been conducted using reef communities with morphologies incorporating multiple scales of roughness (10⁻³ to 10⁻¹ m); however, little attention has been paid to the relative importance of varying roughness scales to total rates of metabolite mass transfer to reef communities. It is well known that autotrophic reef organisms exhibit morphologies that incorporate multiple scales of roughness (Kaandorp 1999). However, the success of correlating nutrient mass-transfer rates to bottom drag or frictional dissipation have led some investigators to suggest that small roughness scales are unimportant to total rates of metabolite mass transfer (Baird and Atkinson 1997; Hearn et al. 2001). In addition, most studies of water motion on coral and algal metabolism have been conducted under steady, unidirection-

al flow. Oscillatory flow resulting from the propagation and transformation of surface gravity waves can dominate the flow environments of many shallow reef communities (Munk and Sargent 1954; Young 1989; Nelson 1996). A few studies have reported enhancements of 15–35% in rates of nitrogen fixation and ammonium uptake by benthic macrophytes under oscillatory versus steady flow (Williams and Carpenter 1998; Thomas and Cornelisen 2003). However, the flows created in those studies were defined by periods too long (>18 s) to include most of the wind waves and swells to which many reef communities are exposed (4–16 s). It is not yet clear to what extent added surface area from multiple roughness scales and thinning of boundary layers under oscillatory flow will affect rates of nutrient mass transfer to coral reef communities living in wave-exposed environments.

The dissolution of plaster has been widely used in aquatic sciences to characterize water motion because plaster dissolution is mass-transfer limited (Muus 1968; Porter et al. 2000). Mass-transfer correlations have been used to accurately predict rates of dissolution of gypsum-coated coral skeletons (Baird and Atkinson 1997). Mass-transfer correlations have also been used to predict rates of phosphate and ammonium uptake by experimental communities of coral, macroalgae, turf-covered coral rubble (Atkinson and Bilger 1992; Larned and Atkinson 1997; Thomas and Atkinson 1997). The dissolution of plaster surfaces can be used as a proxy for the mass transfer of nutrients because the solubility of gypsum in seawater is very high (Krumgalz and Millero 1983) and the diffusivities of the major ions in gypsum (Ca²⁺ and SO₄²⁻) and dissolved inorganic nutrient species (e.g., H₂PO₄⁻, HPO₄²⁻, NH₄⁺, and NO₃⁻) are similar (Li and Gregory 1974).

The purpose of this research was (1) to examine the importance of different roughness scales (10⁻³ to 10⁻¹ m) on rates of mass transfer and (2) to compare rates of mass transfer under steady flow and wave-driven, oscillatory flow.

¹ To whom correspondence should be addressed. Present address: MSB 205, 1000 Pope Road, Honolulu, Hawaii 96822 (falter@hawaii.edu).

Acknowledgments

Thanks to Jim Fleming and Eric Hochberg for suggestions and help in doing field work. This research was supported by the University of Hawaii Sea Grant Program project number R/CR-1 along with a grant from the National Science Foundation number OCE0118172 and the Alliance for Coastal Technology. This is Hawaii Institute of Marine Biology contribution 1188 and School of Ocean and Earth Science and Technology 6440.

These two objectives were addressed by two sets of experiments: one set conducted using a flume and another set conducted on natural reef flats dominated by wave-driven flow. Experiments were performed by constructing plaster forms with simple geometries and allowing these forms to dissolve under various flow conditions. The design of the forms allowed for both repeatability and control of surface morphology, as well as providing a simple and accurate means to quantify surface area.

Background: Mass-transfer theory—An effective description of mass transfer to solid surfaces involving both diffusion and convection is achieved by combining the transport conservation equations with the respective boundary conditions in a formulation analogous to Newton's "law" of cooling for heat transfer. The resulting generalized mass-transfer formulation relates the flux of a species i (J_i in $\text{mmol m}^{-2} \text{d}^{-1}$) to the difference between the concentration of i in the bulk fluid ($C_{i,b}$ in mmol m^{-3}) and at the solid surface ($C_{i,s}$), and the mass-transfer coefficient (S_i in m d^{-1} or m s^{-1})

$$J_i = S_i(C_{i,b} - C_{i,s}) \quad (1)$$

In essence, Eq. 1 relates the transport rates given by the conservation equations (continuity, momentum, and species) in terms of the boundary conditions and a convective mass-transfer coefficient, S . S has the dimensions of velocity and is reported in units of either meters per day or meters per second, and can be expressed as the product of the nondimensional Stanton number (St) and the flow speed of the ambient fluid moving over the surface (U)

$$S = StU \quad (2)$$

St can be thought of as the mass-transfer rate that a surface can support at a given ambient flow speed, i.e., higher St implies greater mass transfer for a given U . St is usually defined based on steady flow speed; however, here we define St based on root-mean square flow speed (U_{rms}) for both steady and oscillatory flows. Based on experimental (Atkinson and Bilger 1992; Baird and Atkinson 1997; Thomas and Atkinson 1997) and theoretical (Bilger and Atkinson 1992; Hearn et al. 2001) mass-transfer relationships for coral reef communities, S has been shown to follow a power-law dependency on U such that $S \propto U^{0.8}$ and $St \propto U^{-0.2}$. Mass-transfer rates for dissolved major ions such as Ca^{2+} and SO_4^{2-} , as well as dissolved nutrients (e.g., NH_4^+ , NO_3^- , and PO_4^{3-}), are characterized by high Schmidt numbers (400–1,500). The Schmidt number (Sc) is a nondimensional quantity defined as the ratio of the kinematic viscosity of the fluid (ν) to the diffusivity of the dissolved species in question ($Sc_i \equiv \nu/D_i$). The dependency of S and St on Sc for $Sc < 4,600$ (Dawson and Trass 1972) is

$$S_i \propto Sc_i^{-0.58} \quad St_i \propto Sc_i^{-0.58} \quad (3)$$

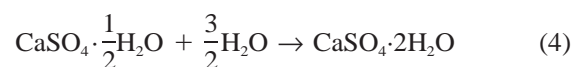
Despite the dependencies of S and St on Sc and U to fractional powers, S still has integer dimensions (m d^{-1}) and St is still unitless because of the fractional power-law dependency of these variables on other empirical, nondimensional, and physical (e.g., density) constants not shown here (Bilger and Atkinson 1992; Falter et al. 2004).

In this study we measure S and St for dissolved calcium

(S_{Ca} and St_{Ca}) based on measurements of plaster dissolution at different flow speeds, both in the flume and in the field (Eqs. 1 and 2).

Methods

Plaster forms were prepared using No. 1 pottery plaster (US Gypsum, percentage by weight, 96.2% β -hemihydrate [$\text{CaSO}_4 \cdot 1/2\text{H}_2\text{O}$], 0.5% CaSO_4 , 2.4% dolomite [$\text{CaMg}(\text{CO}_3)_2$], 0.4% oxides, 0.5% acid insolubles). This composition was checked against an analysis of the material by inductively coupled plasma and optical emission spectroscopy (Baird and Atkinson 1997). The plaster powder was hydrated using tap water to form solid gypsum by the following reaction



The plaster powder was mixed in a 5:4 vol:vol ratio for 1.5 min before being poured into polyvinyl chloride (PVC) molds. The basic plaster form consisted of a smooth-faced, rectangular block $6 \times 6 \times 12 \text{ cm}^3$.

Flume experiments—Smooth plaster blocks were allowed to dissolve in flowing sea water inside a flume. The main body of the flume is a modified U tube constructed from 0.3-m diameter PVC pipe with an internal piston driven by an electric motor (Fig. 1). The test section of the flume is rectangular in cross-section: 0.3 m wide, 0.35 m high, and 3 m long. Transition segments (0.5 m long) on either end of the test section smooth the transition from the circular pipe to the rectangular test section. Oscillating flows from 8 to 47 cm s^{-1} were generated by fixing distinct periods of oscillation (5.2, 7.5, and 11.3 s) and orbital excursion amplitudes (0.3, 0.6, 0.9, and 1.2 m) in various combinations. To generate unidirectional flow, the piston was pulled all the way back from the piston chamber to open the path between the two standpipes and through the test section. Next, a section of 0.3-m diameter pipe was raised to connect the two standpipes. A small electric propeller mounted inside this bridge section was used to drive unidirectional flow. For all experiments, the test section was filled with pieces of coral rubble 10–15 cm high, 15–20 cm wide, and separated by a few centimeters (Fig. 2). One plaster form was mounted on a plate 5 cm off the bottom of the flume in the middle of the test section. Another form was similarly mounted at the downstream end of the test section (Fig. 2). Fresh seawater was allowed to flow into and out of the flume at a rate of $\sim 50 \text{ L min}^{-1}$ throughout the course of all experiments. A Nortek NDV model acoustic Doppler velocimeter (NortekUSA) was mounted 0.4 m downstream of the middle plaster form with only the sensor penetrating the bottom of the test section. Water motion was measured at a point 20 cm off the bottom and at a sampling frequency of 2 Hz.

Field experiments—Field experiments were conducted on three different reef flats in Kaneohe Bay, Oahu, Hawaii (Fig. 3). Plaster forms were constructed with roughness ranging from millimeters to decimeters in scale and allowed to dis-

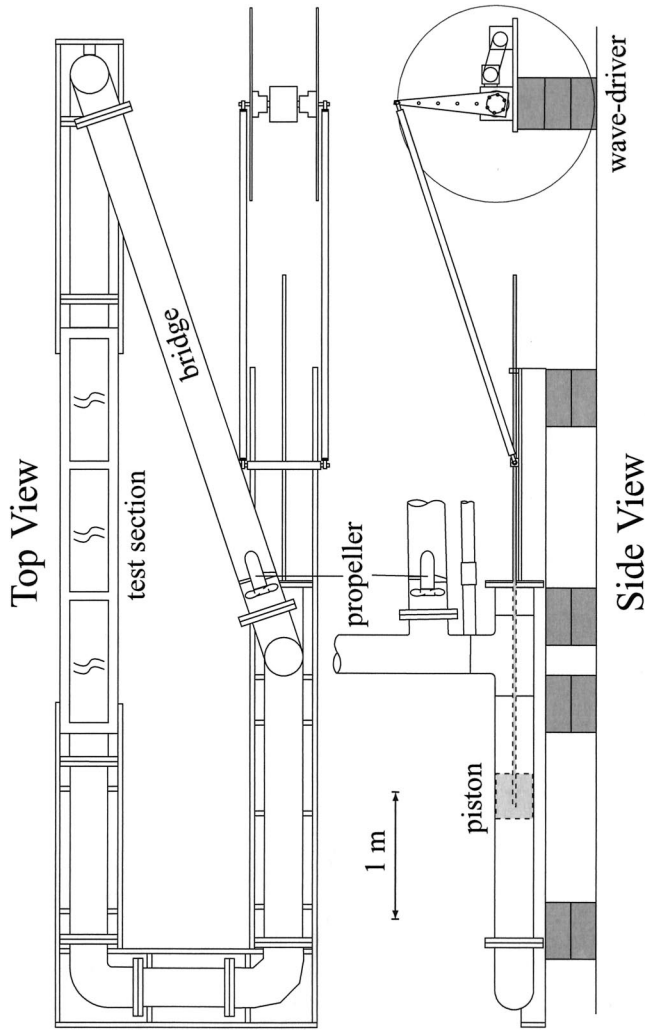


Fig. 1. Schematic of flume from both top and side views. The flume is capable of generating steady flows up to 50 cm s^{-1} and oscillatory flows of up to 50 cm s^{-1} (rms) with periods of 5 to 12 s.

solve under in situ flow conditions at depths $< 2 \text{ m}$. The reef flats permitted the simultaneous deployment of more and larger plaster forms than the flumes. To create decimeter-scale roughness, 8 to 22 individual plaster forms were assembled in a staggered array on square plates 0.4 or 0.5 m in width (Fig. 4, termed plate forms). Elements were uniformly spaced in a staggered array roughly 3–12 cm apart depending on the number of elements arranged on a given plate (Fig. 4A). The bottom of the plate was filled to its rim ($\sim 2 \text{ cm}$) with additional plaster to create a continuous plaster surface. To create centimeter-scale roughness on the plaster forms, cylindrical holes 1-cm wide and 1-cm deep were drilled into all faces of the basic plaster form (Fig. 4B). To create millimeter-scale roughness on the plaster forms, grooves 1.5 mm wide and 2 mm deep were routed at 0.5-cm intervals in all exposed faces of the basic plaster form (Fig. 4B). In addition to plate forms, individual plaster forms of varying surface roughness were dissolved in the field. For all deployments, flow was measured with a MAVS-3 three-dimensional current meter (NOBSKA) sampling at 2 Hz

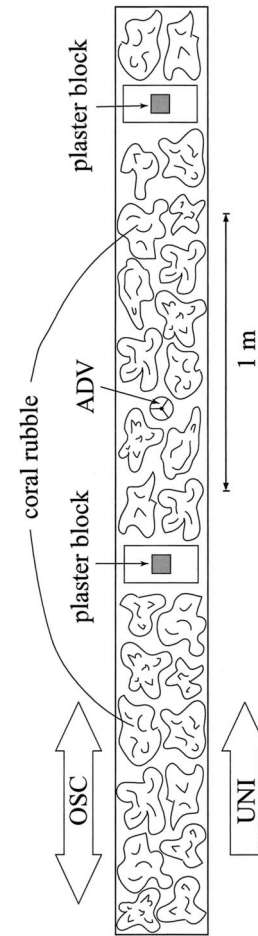


Fig. 2. Diagram of experimental setup in test section. ADV sensor is pointing upward measuring flow 20 cm from the bottom of the flume near the center. The arrows labeled OSC and UNI denote the directions of oscillatory and steady, unidirectional water motion, respectively. The test section is 30 cm wide, 35 cm deep, and 3 m wide. The transition segments bounding either side of the test section are not shown.

with its sensor positioned 0.3 m off the bottom. U_{rms} was calculated using data from the horizontal axes according to

$$U_{\text{rms}} = \sqrt{\langle u^2 + v^2 \rangle_t} \quad (5)$$

where u and v represent flow along the two axes parallel to the bottom and the brackets $\langle \rangle$ represent averaging of these variables with respect to time. The magnitudes of the mean horizontal velocity ($\langle |U| \rangle_t$) were also calculated from the same u - v data according to

$$\langle |U| \rangle_t = \sqrt{\langle u^2 \rangle_t + \langle v^2 \rangle_t} \quad (6)$$

We measured wet weight loss of all plaster forms. To convert the weight loss of wet plaster to the loss of calcium in moles, we determined the ratio of the densities of dry and wet plaster $\rho_{\text{dry}}/\rho_{\text{wet}}$ in the following manner. Two plaster forms from each of three batches of plaster ($n = 6$) were soaked in water for 4 h, allowed to sit for 30 min, and then weighed before being placed in a temperature-controlled oven at 55°C . The forms were then weighed four times over the following 4 d,

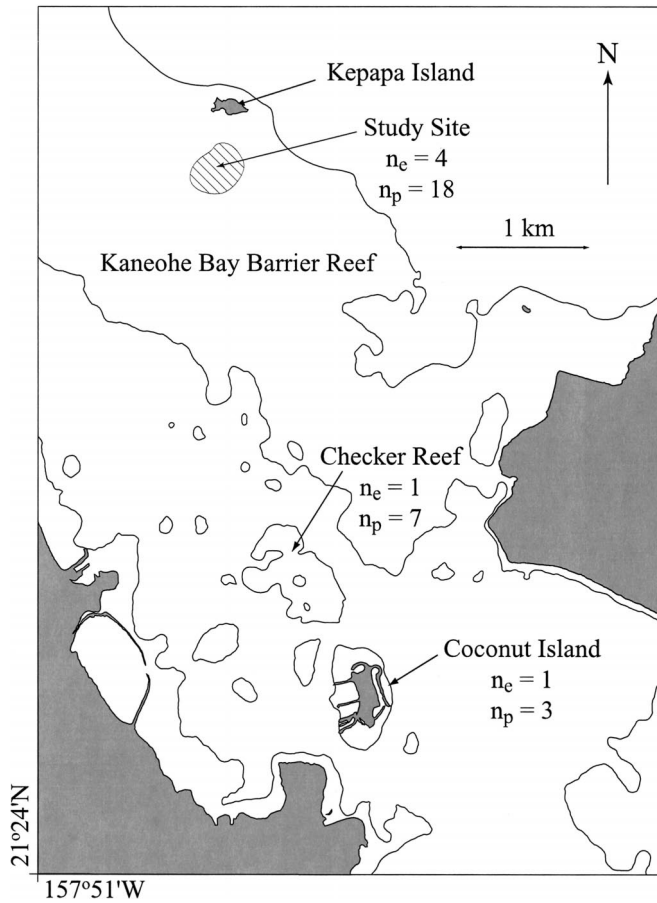


Fig. 3. Map of experimental field sites within the vicinity of Kaneohe Bay. Outlines of the barrier and patch reefs are indicated by the 4-m isobath. Multiple experimental deployments were carried out on the Kaneohe Bay Barrier Reef flat as indicated by the hatched area. The number of experiments (n_e) and plaster forms dissolved (n_p) at each site are also shown.

after which $\rho_{\text{dry}}/\rho_{\text{wet}}$ had reached an asymptotic value of 0.64 ± 0.02 . The mass of plaster lost from dissolution (ΔM_{wet}) could then be converted into the mass of calcium lost in moles (ΔM_{Ca}) by the following equation

$$\Delta M_{\text{Ca}} = \frac{\Delta M_{\text{wet}} \left(\frac{\rho_{\text{dry}}}{\rho_{\text{wet}}} \right)}{MW_{\text{gyp}} \left(\frac{\rho_{\text{dry}}}{\rho_{\text{wet}}} \right)} \quad (7)$$

where MW_{gyp} is the molecular weight of gypsum (172.2 g).

Mass transfer of Ca^{2+} from dissolving gypsum surfaces in sea water—Equation 3 indicates that S_i should be a function of the species diffusivity, D_p , raised to the 0.58 power. D_i is a function of the temperature and salinity of the water (Li and Gregory 1974); therefore, all calculations of S_{Ca} were corrected to a temperature of 25°C according to following expression derived from Eq. 3

$$S_{25} = S_T \left(\frac{D_{25}}{D_T} \right)^{0.58} \quad (8)$$

Diffusivities of Ca^{2+} and SO_4^{2-} were calculated using the

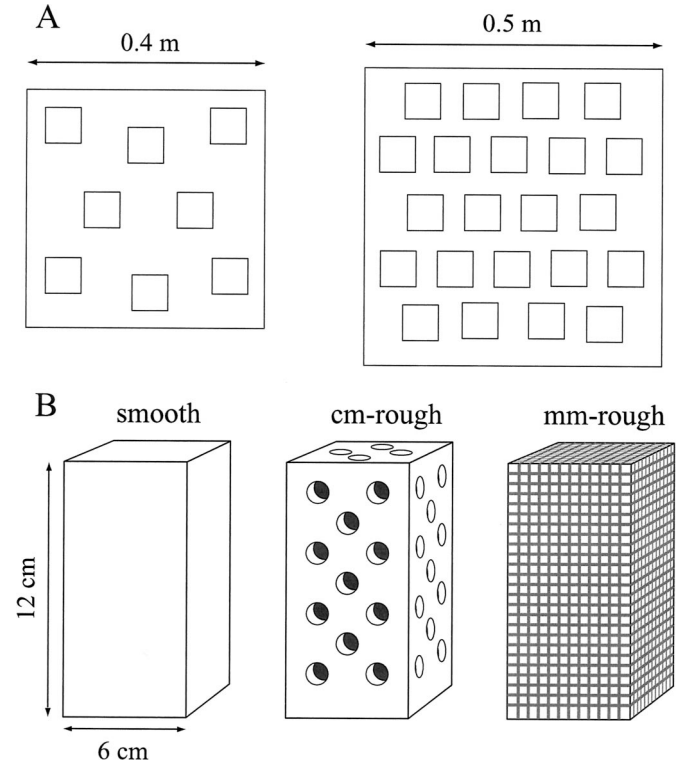


Fig. 4. (A) Schematic of 0.4- and 0.5-m plate form designs with examples of individual plaster form arrangements. (B) Individual plaster forms with smooth faces, centimeter-scale roughness added, and millimeter-scale roughness added.

diffusivities of the free ions and their ion pairs (Li and Gregory 1974) weighted by their relative proportions (Stumm and Morgan 1981) and assuming a constant salinity of 35. Mass-transfer coefficients were estimated from the loss of calcium in moles (ΔM_{Ca}), duration of the experiment (Δt), total surface area of the form (TSA), and the difference in Ca^{2+} concentrations at the plaster surface and in the ambient sea water ($\Delta[\text{Ca}^{2+}]$)

$$S_{\text{Ca}} = \frac{\Delta M_{\text{Ca}}}{\Delta t \Delta[\text{Ca}^{2+}] \text{TSA}} \quad (9)$$

$\Delta[\text{Ca}^{2+}]$ was calculated based on the solubility of gypsum in seawater and the concentration of Ca^{2+} and SO_4^{2-} in seawater at a salinity of 35 and a temperature of 25°C (Pytkowicz and Hawley 1974; Krungalz and Millero 1982, 1983) following methods and assumptions similar to Santschi et al. (1991). The duration of all experiments varied from 2 to 16 h.

Mass-transfer coefficients are conventionally normalized by planar projected area of the active surface. However, all values for S_{Ca} and St_{Ca} in this study were normalized by the total surface area of each plaster form. Total surface areas were calculated as the mean of the surface area before and after an experiment. Ninety-five percent confidence limits for mean surface areas were generated by Monte Carlo simulation of measured uncertainties in the plaster form dimensions: plate width, plate depth, form height, form width, form depth, hole diameter, hole depth, groove width, and

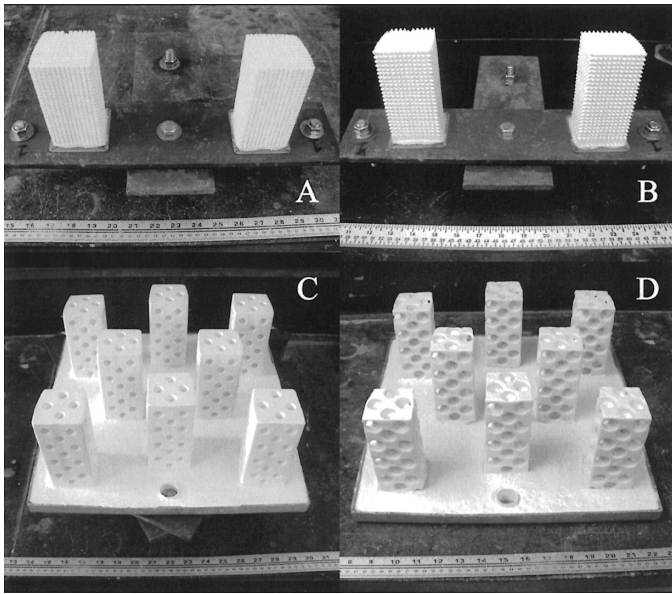


Fig. 5. Individual plaster forms with added millimeter-scale roughness (A) before and (B) after dissolution. Plate forms with added centimeter-scale roughness (C) before and (D) after dissolution.

groove depth. For field experiments, St_{Ca} was calculated from S_{Ca} using U_{rms} as the velocity scale according to Eq. 2. All regressions of S_{Ca} and St_{Ca} against U_{rms} were performed using a nonlinear least-squares procedure in Matlab (the Mathworks). Finally, the thin-film thickness of the concentration boundary layer (δ_c) was estimated from S_{Ca} and the surface area of the plaster form according to Eq. 1 and Fick's first law of diffusion

$$\delta_c \approx \frac{D_{\Sigma Ca}}{S_{Ca}} \quad (10)$$

where $D_{\Sigma Ca}$ is the weighted diffusivity of all Ca^{2+} species in seawater (Li and Gregory 1974; Stumm and Morgan 1981).

Results

Changes in form morphology—Following dissolution of plaster forms in the field and flume, total surface area changed $<10\%$ for all forms except for the grooved forms, for which surface area changed 15–30%; thus, there was little physical deformation of plaster forms (Fig. 5). The calculated uncertainty in surface area estimates was greatest for the grooved forms ($\pm 10\%$), followed by elements and forms with holes ($\pm 6\%$), and then the smooth forms ($\pm 3\%$). Uncertainties in estimates of calcium loss were 2–10%, with the greatest uncertainty for the forms and elements with the lowest surface area (i.e., the smooth forms).

Flume experiments—Water temperatures varied from 26.5°C to 28°C between all flume experiments, but only a few tenths of a degree over the course of a single experiment. Flow speeds (U_{rms}) in the flume ranged from 7 to 43 $cm\ s^{-1}$. Calcium mass-transfer coefficients were positively

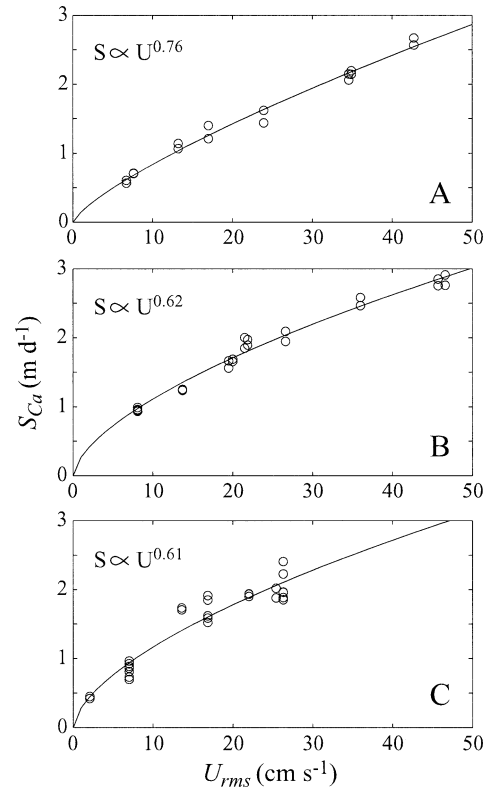


Fig. 6. S_{Ca} versus U_{rms} for (A) steady, unidirectional flow in the flume (B) oscillatory flow in the flume, and (C) all flows in the field. All data were fit with power-law relationships ($S_{Ca} = aU_{rms}^b$). The regression equations shown are (A) $S_{Ca} = 4.9U_{rms}^{0.76}$, $r^2 = 0.98$, $n = 16$; (B) $S_{Ca} = 4.6U_{rms}^{0.62}$, $r^2 = 0.98$, $n = 22$; and (C) $S_{Ca} = 4.7U_{rms}^{0.61}$, $r^2 = 0.92$, $n = 22$. The 95% confidence limits for each of the best-fit exponents are (0.70, 0.83) for steady flow in the flume (A), (0.57, 0.66) for oscillatory flow in the flume (B), and (0.51, 0.71) for flow in the field (C).

correlated with U_{rms} under both steady and oscillatory flow and followed a simple, power-law relationship (Figs. 6A,B). The dependency of S_{Ca} on U_{rms} under steady flow was similar to experimental (Atkinson and Bilger 1992; Baird and Atkinson 1997; Thomas and Atkinson 1997) and theoretical (Bilger and Atkinson 1992; Hearn et al. 2001) mass-transfer relationships for reef communities ($S \propto U^{0.8}$, Fig. 7). However, the exponential dependency of S_{Ca} on U_{rms} under oscillatory flow was significantly lower than under steady flow ($S_{Ca} \propto U^{0.62}$ vs. $S_{Ca} \propto U^{0.76}$, two-way t -test, $p < 0.005$, $n = 16$ and $n = 22$). Plotting St_{Ca} versus U_{rms} provides a better visual comparison of mass-transfer rates under different flow conditions than S_{Ca} versus U_{rms} by removing some of the dependency of mass-transfer rates on flow speed (Fig. 8A). Rates of plaster dissolution were higher under oscillatory flow than under steady flow. We define the enhancement of mass transfer under oscillatory flow over steady flow (E_{osc}) to be the ratio of S_{Ca} (S_{osc}/S_{steady}) at a given U_{rms} . E_{osc} increased quasi-linearly with decreasing U_{rms} from <1.1 for $U_{rms} > 40$ $cm\ s^{-1}$ to 1.3 for $U_{rms} = 10$ $cm\ s^{-1}$ before increasing more nonlinearly to roughly 1.5 for $U_{rms} = 5$ $cm\ s^{-1}$ (Fig. 8B).

Field experiments—Water temperatures varied between 23°C and 27°C over all field deployments, leading to tem-

perature-dependent corrections in S_{Ca} and St_{Ca} of between $\pm 5\%$. U_{rms} in the field varied between 2 and 26 cm s^{-1} . Mean horizontal velocity $\langle U \rangle$ is a vector quantity representing the net water movement in a given direction over a period of time and is different from U_{rms} , which is a scalar quantity representing the average magnitude of the speed of the flow. Under purely steady flow, $\langle U \rangle = U_{rms}$ while under purely oscillatory flow, $\langle U \rangle = 0$. Therefore, the ratio of $\langle U \rangle$ to U_{rms} should go from 0 to 1 as a flow goes from being purely oscillatory to being mixed steady + oscillatory and then to being purely steady. Values of $\langle U \rangle$ were $< 15\%$ of U_{rms} for $U_{rms} > 10 \text{ cm s}^{-1}$, reflecting the dominance of wave kinematics under these flow conditions; however, $\langle U \rangle$ was 40–50% of U_{rms} for $U_{rms} < 10 \text{ cm s}^{-1}$, indicating more mixed flow conditions. Peak periods in the flow spectra occurred between 7 and 10 s, reflecting trade wind-generated waves; however, there was significant energy at higher frequencies, or shorter periods, in each of the spectra (data not shown). This is indicative of the multispectral nature of natural, wave-driven flow conditions. Rates of plaster dissolution obtained in the field were not significantly different from rates of plaster dissolution under oscillatory flow in the flume ($< 10\%$ difference between predicted values), even when comparing the mixed, low-flow conditions in the field (Figs. 6B,C). Finally, all rates of dissolution in the field were linearly proportional to surface area regardless of the roughness scale ($\text{mol Ca d}^{-1} = 104 \times \text{TSA} - 0.5$, Fig. 9).

The effective thin-film thickness of the concentration boundary layer, δ_c , varied between 20 and 160 μm for all field and flume experiments and decreased with increasing velocity (Fig. 10).

Discussion

Rectangular forms as analogs for complex shapes—The rectangular plaster forms used in this experiment showed a dependency on unidirectional flow speed similar to that of prior experimental communities and other mass-transfer studies, where $S \propto U^{0.8}$ and $St \propto U^{-0.2}$. Thus, these simple plaster forms are good analogs for the more complex morphologies of reef communities.

Importance of oscillatory flow—In order to compare rates of mass transfer under different flow conditions, it is necessary to choose a common velocity scale upon which to make these comparisons. Flow parameters that separately describe the mean flow, the time-variant component of the flow, or a ratio of these parameters, do not provide good bases for comparing mass-transfer rates (Williams and Carpenter 1998; Porter et al. 2000; Thomas and Cornelisen 2003). We chose rms-flow speed as an appropriate velocity scale because it provides a measure of total water motion, regardless of whether the flow is steady or oscillatory. We found measured rates of mass transfer that were up to 50% higher under oscillatory flow than under steady flow. If the time-average flow speed $\langle U \rangle$, were used as the comparative velocity scale, then measured enhancement would be up to 60% because the ratio of U_{rms} to $\langle U \rangle$, is ~ 1.1 for quasi-sinusoidal flow. It is not surprising that enhancement was greatest at the lowest flow speeds, given that St becomes

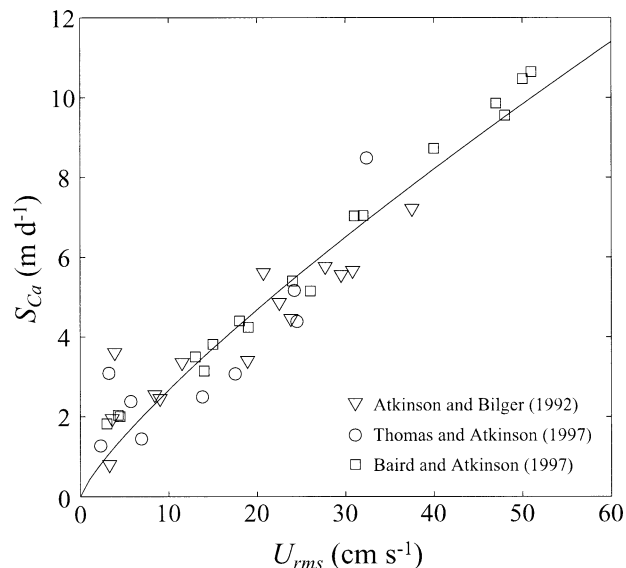


Fig. 7. Plot of mass-transfer coefficients based on data from Atkinson and coworkers (see figure legend). All values have been normalized to a Sc for Ca^{2+} in seawater at a temperature of 25°C and a salinity of 35 (see text for details). Regression shown is $S_{Ca} = 17.9U_{rms}^{0.81}$, $r^2 = 0.91$, $n = 39$.

increasingly sensitive to changes in flow speed as flow speed decreases (Baird and Atkinson 1997; Thomas and Atkinson 1997; this study). Consequently, modest changes in U_{rms} can lead to more pronounced changes in St and S . This sensitivity also implies that predicting mass-transfer rates for benthic organisms and communities will be most difficult at low flow speeds.

Our results are consistent with observed enhancement under oscillatory flow in rates of nitrogen fixation and ammonium uptake by benthic macrophytes (Williams and Carpenter 1998; Thomas and Cornelisen 2003). There must be some mechanism occurring under oscillatory flow that is augmenting mass-transfer rates. One possible mechanism is that turbulence created by the coral rubble was higher under oscillatory than under steady flow and, through interaction with the plaster forms, resulted in an increase in mass-transfer rates (Hearn et al. 2001; Thomas and Cornelisen 2003). Although we did not quantify turbulence in the present study, the dissolution of plaster forms under steady flow in an empty flume was $\sim 20\%$ lower than in a flume filled with coral rubble, demonstrating how the removal of turbulence-generating roughness can potentially alter mass-transfer rates ($U_{rms} \approx 20 \text{ cm s}^{-1}$, data not shown). Proper identification of the fluid mechanisms responsible for differences in mass-transfer rates under steady and nonsteady flow will require a more detailed examination of flow near active surfaces than we have performed here.

Mass-transfer rates varied by a factor of ~ 5 within the range of flow conditions observed on reef flat environments ($2\text{--}26 \text{ cm s}^{-1}$). Wave-driven flow speeds greater than 40 cm s^{-1} have been observed on the Kaneohe Bay Barrier Reef flat by other investigators (Williams and Carpenter 1998). Wave-driven currents on the reef flats of Enewetak Atoll, Marshall Islands, commonly reach over 100 cm s^{-1} (Atkin-

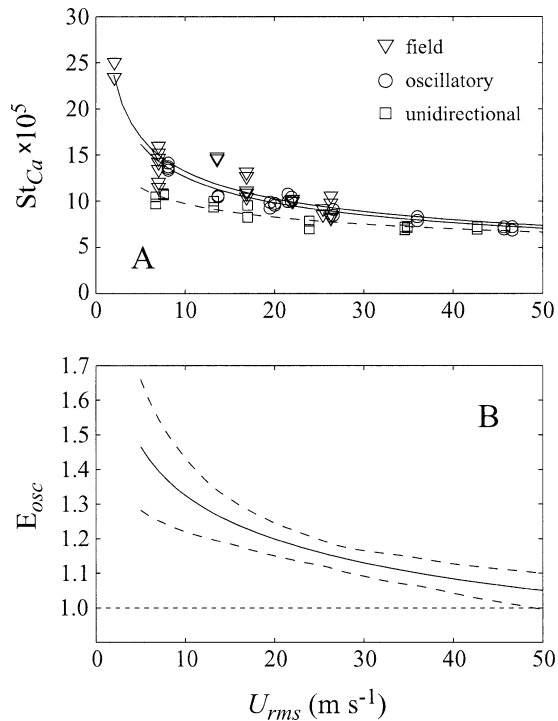


Fig. 8. (A) St_{Ca} versus U_{rms} under steady and oscillatory flow in the flume and flow in the field. All data were fit with power-law relationships ($St_{Ca} = aU_{rms}^b$). The upper solid line represents the best fit for all field data ($St_{Ca} = 5.7U_{rms}^{-0.36}$, $r^2 = 0.90$, $n = 22$), the lower solid line represents the best fit for oscillatory flow in the flume ($St_{Ca} = 5.5U_{rms}^{-0.36}$, $r^2 = 0.95$, $n = 22$), and the bottom dashed line represents the best fit for unidirectional flow in the flume ($St_{Ca} = 5.7U_{rms}^{-0.23}$, $r^2 = 0.86$, $n = 16$). (B) Plot of the wave enhancement on mass-transfer rates (E_{osc} , solid line) versus U_{rms} based on the best-fit regressions in Fig. 6. Calculation of the 95% confidence limits for E_{osc} (dashed lines) come from a Monte Carlo simulation of the error between observed values of S_{Ca} and regression predictions. The dotted line at $E_{osc} = 1$ represents no enhancement.

son et al. 1981). These observations along with our results indicate that S must vary by more than a factor of 10 across coral reefs just from variations in the magnitude of the mean flow. Thus, spatial variation in S is much greater than differences in S between steady and oscillatory flow. Whether flow is steady or oscillatory is important for assessing the mass-transfer characteristics of a specific organism or community in a given locale, but much less important for understanding variations in nutrient uptake over entire coral reef ecosystems. In this sense, the importance of wave-enhancement of mass transfer to the ecology of coral reef communities depends upon the perspective with which it is viewed.

Effect of roughness scale on mass transfer—The simplest explanation for the linear relationship between S_{Ca} and total surface area is that all roughness scales considered in this experiment (0.1–10 cm) exceeded the range in the thickness of the concentration boundary layer (20–160 μm , Fig. 10). Surface area arising from even the smallest roughness scales would not be smoothed out by the concentration boundary layer. As a result, all surfaces on all of the plaster forms

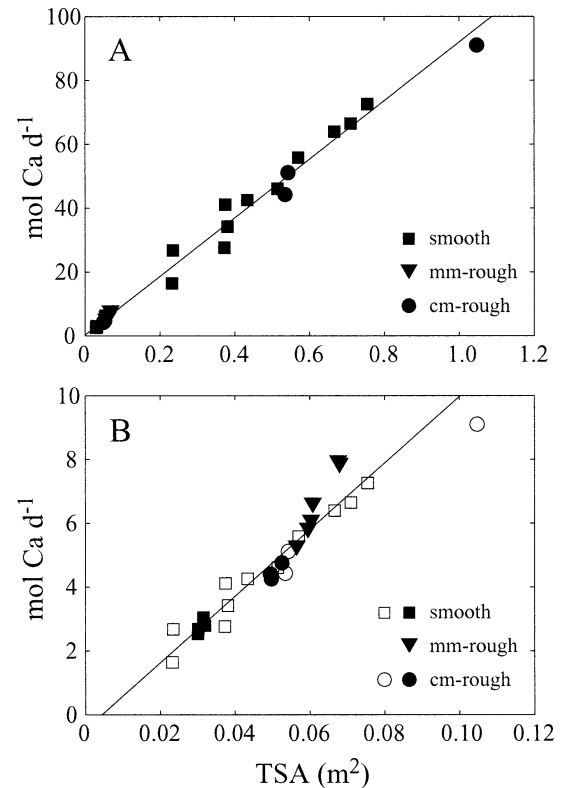


Fig. 9. (A) Rates of plaster dissolution versus total surface area (TSA) for plaster forms of varying roughness scale deployed in the field. Rates shown have been normalized by $U_{rms}^{0.61}$ to remove variations due to flow speed (see text). Line shown ($\text{mol Ca d}^{-1} = 104 \times \text{TSA} - 0.5$, $r^2 = 0.99$, $n = 28$) represents model II regression fit to all the data. (B) Same plot as in (A) but with dissolution rates for plate forms (open symbols) scaled by 1/10 to better compare results with individual forms (solid symbols). Line shown ($\text{mol Ca d}^{-1} = 92 \times \text{TSA} + 0.3$, $r^2 = 0.92$, $n = 28$) represents model II regression fit to all the data.

were equally available for mass transfer regardless of the roughness scale from which they were derived. Still, in order for S_{Ca} to be proportional to surface area, all surfaces would need to be exposed to comparable flow conditions. It is likely that there was sufficient turbulence to transport momentum throughout all roughness elements, thereby minimizing flow stagnation in more recessed areas and its inhibitory effects on mass-transfer rates. This could further explain why there were no interference effects from the proximity—or packing density—of individual plaster forms onto plates. Plate forms dissolved evenly and in a regular fashion (Fig. 5), and dissolution was linearly proportional to total surface area over a 50-fold range (0.02 to 1 m², Fig. 9). Rates of dissolution were also linearly proportional to the ratio of total surface area to projected planar area for the 13 plate forms (Fig. 11), further demonstrating there were no interference effects from the addition of multiple-scale roughness. Ultimately, there may be limits to branch spacing or roughness element proximity for which mass-transfer inhibition due to flow stagnation occurs; however, we did not find those limits within our experimental design.

Prior studies have shown how mass-transfer correlations

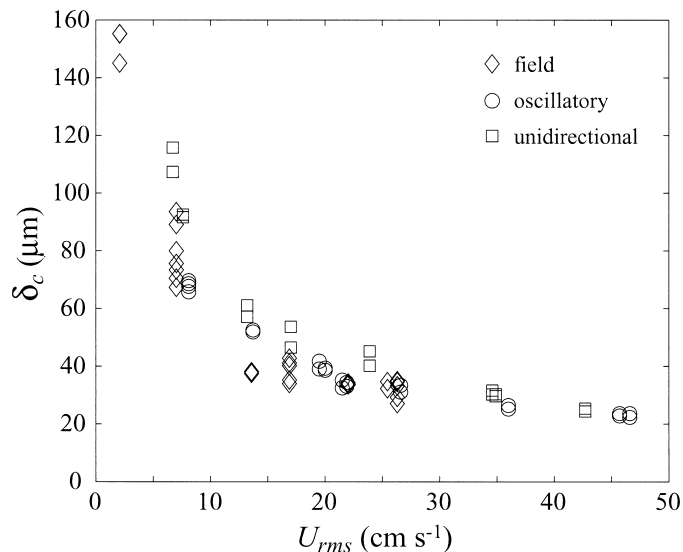


Fig. 10. Effective thin-film thickness of the concentration boundary layer versus U_{rms} under steady, unidirectional flow in the flume (squares), under oscillatory flow in the flume (circles), and in the field (diamonds).

can successfully predict rates of mass transfer based on the frictional roughness of benthic communities (Bilger and Atkinson 1992; Baird and Atkinson 1997; Thomas and Atkinson 1997). This success led Baird and Atkinson (1997) to assert that small-scale roughness features were unimportant to rates of mass transfer because the largest roughness scale is responsible for generating most of the drag exerted by the community on the flowing water. Our data indicate that small-scale roughness features are equally important in determining the total rate of mass transfer to a rough surface. One hypothesis for reconciling these different points of view is that turbulence created primarily by large-scale roughness controls mass-transfer rates to coral reef communities by setting the thickness of the concentration boundary layer (Hearn et al. 2001); however, mass transfer still occurs to surfaces resulting from all roughness scales. It is likely that benthic communities that exhibit greater topographical relief and, therefore, greater drag (Atkinson 1999) will also generally support greater total surface area available for mass transfer.

Bilger and Atkinson (1992) suggested that the ratio of total surface area (TSA) to planar projected area (PPA), which they called α , was not an important parameter upon which rates of nutrient mass transfer to reef communities would depend. Our data indicate that this is not the case. S measured for dissolved calcium, ammonium, and phosphate by Atkinson and coworkers were normalized to PPA (1) in order to be consistent with decades of reef community metabolism and biogeochemical flux measurements that were also normalized to PPA and (2) because measuring PPA for either a natural or experimental reef community is operationally much easier and more reliable than measuring TSA (Hoegh-Goldberg 1988). All S_{Ca} reported here were normalized to TSA to explicitly control for the effects of TSA from multiple roughness scales on mass-transfer rates under dif-

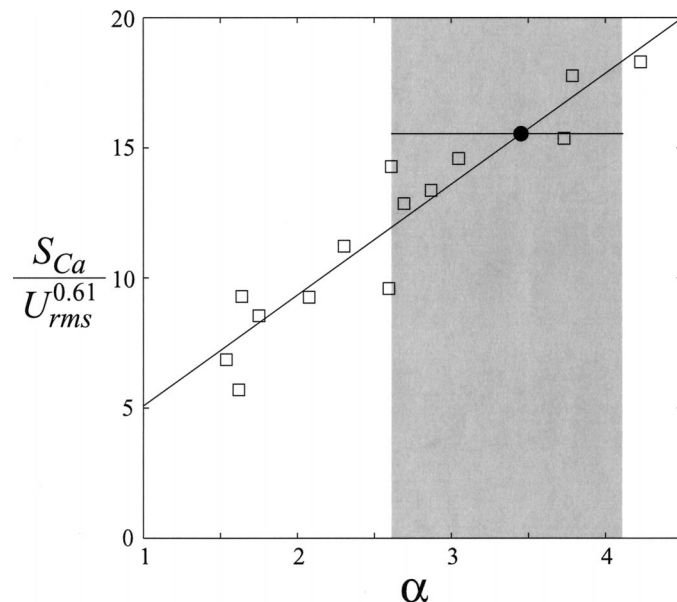


Fig. 11. Calcium mass-transfer coefficients (S_{Ca}) from all plate forms (squares) normalized to planar projected area versus α , or the ratio of total to projected planar surface area ($\alpha \equiv \text{TSA}/\text{PPA}$). S_{Ca} has been normalized by $U_{rms}^{0.61}$ to remove variability due to flow speed. Line shown is $S_{Ca}/U_{rms}^{0.61} = 4.3\alpha + 0.8$, $r^2 = 0.89$, $n = 14$. Applying this regression to the data of Atkinson and coworkers indicates α for their reef communities varied from 2.5 to 4 (shaded area) with a mean of 3.5 (solid circle).

ferent flow conditions. Relationships between S_{Ca} and TSA obtained here suggest that α for the experimental communities used by Atkinson and coworkers varied between 2.5 and 4 (Fig. 11). Although α was not directly measured for these communities, an α of 3.5 for a branching coral (*Stylophora pistillata*) similar in size to those used by Atkinson and coworkers was calculated from direct millimeter-scale measurements of skeletal morphology using computed axial tomography (CAT) scans (S. Chang and S. Monismith pers. comm.). These cursory results indicate that mass-transfer rates to the experimental communities used by Atkinson and coworkers exhibited a similar dependency on surface area as did the plaster forms presented here. It is possible that natural reef communities exhibit a relatively narrow range of α , perhaps 2.5 to 5, thus confining variation in S due to TSA (Fig. 11).

If multiple scales of roughness are equally important for determining total rates of mass transfer, then benthic organisms can maximize their ability to take up nutrients and exchange gasses per unit biomass by adopting morphologies that incorporate multiple scales of roughness. This basic design connotes a tendency for communities to achieve a maximum roughness that optimizes the exchange of materials between them and the water.

We conclude two general points from this research. First, mass transfer is enhanced by as much as 30% to 60% under oscillatory flow over steady flow; however, this enhancement is relatively minor when compared with variation in mass-transfer rates resulting from the more than 10-fold variation in mean flow speeds known to occur across coral reefs (cen-

timeters to decimeters per second). Second, mass transfer is proportional to surface area from decimeter down to millimeter scales, scales that are relevant to the morphologies of coral reef organisms and communities.

References

- ATKINSON, M. J. 1999. Topographical relief as a proxy for friction factors of reefs: Estimates of nutrient uptake into coral reef benthos. p. 28–32. *In* J. E. Maragos and R. Grober-Dunsmore [eds.], Proceedings of the Hawaii Coral Reef Monitoring Workshop. State of Hawaii Department of Aquatic Resources.
- , AND R. W. BILGER. 1992. Effect of water velocity on phosphate uptake in coral reef-flat communities. *Limnol. Oceanogr.* **37**: 273–279.
- , S. V. SMITH, AND E. D. STROUP. 1981. Circulation in Enewetak Atoll lagoon. *Limnol. Oceanogr.* **26**: 1074–1083.
- BAIRD, M. E., AND M. J. ATKINSON. 1997. Measurement and prediction of mass transfer to experimental coral reef communities. *Limnol. Oceanogr.* **42**: 1685–1693.
- BILGER, R. W., AND M. J. ATKINSON. 1992. Anomalous mass transfer of phosphate on coral reef flats. *Limnol. Oceanogr.* **37**: 261–272.
- CARPENTER, R. C., J. M. HACKNEY, AND W. H. ADEY. 1991. Measurements of primary productivity and nitrogenase activity of coral reef algae in a chamber incorporating oscillatory flow. *Limnol. Oceanogr.* **36**: 40–49.
- DAWSON, D. A., AND O. TRASS. 1972. Mass transfer at rough surfaces. *Int. J. Heat Mass Transfer* **15**: 1317–1336.
- DENNISON, W. C., AND D. J. BARNES. 1988. Effect of water motion on coral photosynthesis and calcification. *J. Exp. Mar. Biol. Ecol.* **115**: 67–77.
- FALTER, J. L., M. J. ATKINSON, AND M. A. MERRIFIELD. 2004. Mass transfer limitation of nutrient uptake by a wave-dominated reef flat community. *Limnol. Oceanogr.* **49**: 1820–1831.
- HEARN, C. J., M. J. ATKINSON, AND J. L. FALTER. 2001. A physical derivation of nutrient-uptake rates in coral reefs: Effects of roughness and waves. *Coral Reefs* **20**: 347–356.
- HOEGH-GOLDBERG, O. 1988. A method for determining the surface area of corals. *Coral Reefs* **7**: 113–116.
- KAANDORP, J. A. 1999. Morphological analysis of growth forms of branching marine sessile organisms along environmental gradients. *Mar. Biol.* **134**: 295–306.
- KRUMGALZ, B. S., AND F. J. MILLERO. 1982. Physico-chemical studies of the Dead Sea waters. I. Activity coefficients of major ions in Dead Sea water. *Mar. Chem.* **11**: 209–222.
- , AND ———. 1983. Physico-chemical study of dead sea waters. III. On gypsum saturation in Dead Sea waters and their mixtures with Mediterranean Sea water. *Mar. Chem.* **13**: 127–139.
- LARNED, S. T., AND M. J. ATKINSON. 1997. Effects of water velocity on NH_4 and PO_4 uptake and nutrient-limited growth in the macroalgae *Dictyosphaeria cavernosa*. *Mar. Ecol. Prog. Ser.* **157**: 295–302.
- LI, Y.-H., AND S. GREGORY. 1974. Diffusion of ions in sea water and in deep-sea sediments. *Geochim. Cosmochim. Acta* **38**: 703–714.
- MUNK, W. H., AND M. C. SARGENT. 1954. Adjustment of Bikini Atoll to ocean waves, p. 275–280. U.S. Geol. Surv. Report.
- MUUS, B. 1968. A field method for measuring “exposure” by means of plaster balls, a preliminary account. *Sarsia* **34**: 61–68.
- NELSON, R. C. 1996. Hydraulic roughness of coral reef platforms. *Appl. Ocean Res.* **18**: 265–274.
- PORTER, E. T., L. P. SANFORD, AND S. E. SUTTLES. 2000. Gypsum dissolution is not a universal indicator of “water motion.” *Limnol. Oceanogr.* **45**: 145–158.
- PYTKOWICZ, R. M., AND J. E. HAWLEY. 1974. Bicarbonate and carbonate ion-pairs and a model of seawater at 25 degrees C. *Limnol. Oceanogr.* **19**: 223–234.
- SANTSCHI, P. H., R. F. ANDERSON, M. Q. FLEISHER, AND W. BOWLES. 1991. Measurements of diffusive sublayer thickness in the ocean by alabaster dissolution, and their implications for the measurement of benthic fluxes. *J. Geophys. Res.* **96**: 10,641–10,657.
- STUMM, W., AND J. J. MORGAN. 1981. Aquatic chemistry, 2nd ed. John Wiley & Sons.
- THOMAS, F. I. M., AND M. J. ATKINSON. 1997. Ammonium uptake by coral reefs: Effects of water velocity and surface roughness on mass transfer. *Limnol. Oceanogr.* **42**: 81–88.
- , AND C. D. CORNELISEN. 2003. Ammonium uptake by seagrass communities: Effects of oscillatory versus unidirectional flow. *Mar. Ecol. Prog. Ser.* **247**: 51–57.
- WILLIAMS, S. L., AND R. C. CARPENTER. 1988. Nitrogen-limited primary productivity of coral reef algal turfs: Potential contribution of ammonium excreted by *Diadema antillarum*. *Mar. Ecol. Prog. Ser.* **47**: 145–152.
- , AND ———. 1998. Effects of unidirectional and oscillatory water flow on nitrogen fixation (acetylene reduction) in coral reef algal turfs, Kaneohe Bay, Hawaii. *J. Exp. Mar. Biol. Ecol.* **226**: 293–316.
- YOUNG, I. R. 1989. Wave transformations over coral reefs. *J. Geophys. Res.* **94**: 9779–9789.

Received: 7 March 2004

Accepted: 3 August 2004

Amended: 14 September 2004